

# Porous structured vanadium oxide electrode material for electrochemical capacitors

Ravinder N. Reddy, Ramana G. Reddy\*

*Department of Metallurgical and Materials Engineering, University of Alabama, P.O. Box 870202, Tuscaloosa, AL 35487-0202, USA*

Received 14 April 2005; accepted 10 May 2005

Available online 1 August 2005

## Abstract

A nano porous vanadium oxide ( $V_2O_5$ ) was prepared by sol–gel method. The preparation involved elutriation of aqueous sodium meta vanadate over a cation exchange resin. The product was characterized using X-ray diffraction, scanning electron microscopy, energy dispersive spectroscopy, surface area analysis and thermogravimetric analysis. Electrochemical characterization was done using cyclic voltammetry in a three electrode system consisting of a saturated calomel electrode as reference electrode, platinum mesh as a counter electrode, and  $V_2O_5$  mounted on Ti mesh as the working electrode. Two molar of aqueous KCl, NaCl and LiCl were used as electrolytes. A maximum capacitance of  $214 \text{ F g}^{-1}$  was obtained at a scan rate of  $5 \text{ mV s}^{-1}$  in 2 M KCl. The effect of different electrolytes and the effect of concentration of KCl on the specific capacitance of  $V_2O_5$  were studied. Specific capacitance faded rapidly over 100 cycles in 2 M KCl at a  $5 \text{ mV s}^{-1}$  scan rate.

© 2005 Elsevier B.V. All rights reserved.

**Keywords:** Porous materials; Sol–gel;  $V_2O_5$ ; Electrochemical capacitors

## 1. Introduction

Electrochemical capacitors (ECs) are charge storage devices. ECs stand in between batteries and conventional capacitors in terms of energy density. They are being used in back-up memory applications for many electronic devices. A promising future application of this electrochemical device is in hybrid electric vehicles in conjunction with a battery or fuel cell. In such a combination, the role of the EC is to provide peak power during starting and up hill driving. As a result there is high requirement for high power density ECs. Pseudocapacitors are one of the classifications of electrochemical capacitors and are being investigated for high power applications [1–10]. An electrode material, which is economic, porous and can exist in several oxidation states, is preferred for high power density applications. A highly porous material can utilize the electrolyte effectively at high

power requirements and can be charged and discharged quickly. One of the easiest ways of making such an electrode material is by the sol–gel method. The sol–gel method has several advantages. Transition metal oxide powders can be prepared in homogenous, highly porous and high purity form and with particle sizes in submicron range.

Amorphous  $\text{RuO}_2 \cdot x\text{H}_2\text{O}$  is an ideal electrode material for a pseudocapacitor with a specific capacitance of  $720 \text{ F g}^{-1}$ . However,  $\text{RuO}_2 \cdot x\text{H}_2\text{O}$  is very expensive. Efforts are being made to find a suitable material to replace  $\text{RuO}_2$ .  $V_2O_5$  seems to be a viable electrode material for a pseudocapacitor because of its low cost and vanadium exists in different oxidation states. Very few investigations were performed on  $V_2O_5$  as an electrode material for a pseudocapacitor [11–13]. Lee et al. prepared  $V_2O_5$  by quenching  $V_2O_5$  fine powders at  $950^\circ\text{C}$  into a bath of deionized water [11]. They studied this electrode material in an aqueous KCl electrolyte. The material showed an ideal capacitance curve under cyclic voltammetric conditions. They reported a specific capacitance of  $346 \text{ F g}^{-1}$  at a pH of 2.32 and studied only up to 100 charge/discharge

\* Corresponding author. Tel.: +1 205 348 1740; fax: +1 205 348 2164.  
E-mail address: [rreddy@coe.eng.ua.edu](mailto:rreddy@coe.eng.ua.edu) (R.G. Reddy).

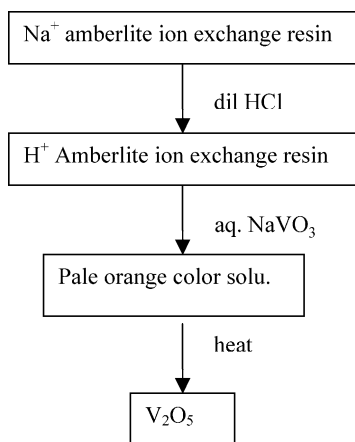


Fig. 1. Schematic representation of  $V_2O_5$  powder synthesis.

cycles. Kudo et al. synthesized a  $V_2O_5$  sol by reacting metallic vanadium with 30%  $H_2O_2$  [13]. They studied  $V_2O_5$  and carbon composite electrodes in non-aqueous electrolytes. This material did not show ideal capacitance and the authors did not mention the specific capacitance ( $F\ g^{-1}$ ) in their paper. In this paper we report highly porous layered  $V_2O_5$  as an electrode material for ECs in different neutral electrolytes.

## 2. Experimental

An aqueous solution of sodium meta vanadate ( $NaVO_3$ ) was passed through a cation exchange resin. The resin used was Amberlite IR 120 plus (Alfa). The resin was in sodium form which was converted to the  $H^+$  form by elutriating with dilute hydrochloric acid. A pale yellow color vanadic acid was collected in a beaker after passing aqueous  $NaVO_3$  through the acidic form of the resin. The pale yellow solution was heated to produce orange colored vanadium oxide powders. A schematic representation of  $V_2O_5$  powder synthesis is shown in Fig. 1.

## 3. Characterization

$V_2O_5$  powders were characterized using X-ray diffractometry (XRD), scanning electron microscopy (SEM), energy dispersive spectroscopy (EDS) and thermogravimetric analysis (TGA). XRD was performed using a Philips PW3830 model. Particle size and morphology were analyzed using the Philip XL30 scanning electron microscope. TGA was performed using Perkin-Elmer Pyris Diamond with a temperature increment of  $10\ ^\circ C\ min^{-1}$  under ambient conditions. The TGA was used to find the amount of water present and also study the structural transformations of  $V_2O_5$ . Surface area was determined by Brunauer–Emmet–Teller (BET) method using NOVA 1200 from Quanta Chrome. Initially, the sample was vacuum degassed for several hours at  $120\ ^\circ C$  under the flow of nitrogen before the BET measurement.

## 3.1. Electrode preparation and electrochemical characterization

Prepared powders were mixed with 25 wt.% of acetylene black and 5 wt.% of PTFE binder. The mixture was mixed using mortar and pestle and pressed to make thin sheets. The sheets were rolled to get approximate thickness of  $100\ \mu m$ . The electrode material was pressed on to titanium mesh by means of roller. The weight of the electrode material in every experiment was approximately 10 mg. Cyclic voltammetry (CV) was conducted using an EG&G potentiostat and galvanostat 273A employing a three electrode experimental setup. Platinum mesh and saturated calomel electrode were used as the counter and reference electrodes respectively. The electrolytes used in this study were  $NaCl$ ,  $KCl$ ,  $LiCl$  and with varying concentration. A voltage range of  $-0.2$  to  $0.7\ V$  and varying scan rate were employed. Specific capacitance ( $F/g$ ) is calculated as the average anodic current ( $-0.1$  to  $0.7\ V$ ) divided by the scan rate and is normalized to 1 g of active material.

## 4. Results and discussion

Fig. 2 shows the XRD pattern of  $V_2O_5$  powders. The pattern shows one dimensional layered type structure evident by intensity peaks at regular intervals. This type of structure was observed by Huguenin et al. in their preparation of  $V_2O_5$  from vanadyl tris(isopropoxide) and water using sol–gel method [14]. Fig. 3 shows TGA curves of  $V_2O_5$  powders in the temperature range of  $30$ – $800\ ^\circ C$ , which depict typical water loss behavior. The TGA curve showed a total weight loss of 16% in the given temperature range. Water loss of around 11% was observed until  $200\ ^\circ C$  and no phase transition was observed until the melting point ( $614\ ^\circ C$ ). Fig. 4 shows an SEM micrograph of  $V_2O_5$  powders. A highly porous nano size honey comb structure with an average pore size of 400 nm and wall thickness of 150 nm can be observed from the micrograph. This kind of morphology is preferred

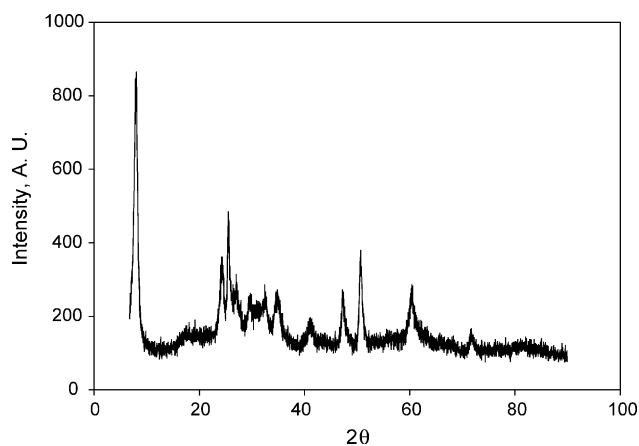


Fig. 2. XRD pattern of  $V_2O_5$  powders.

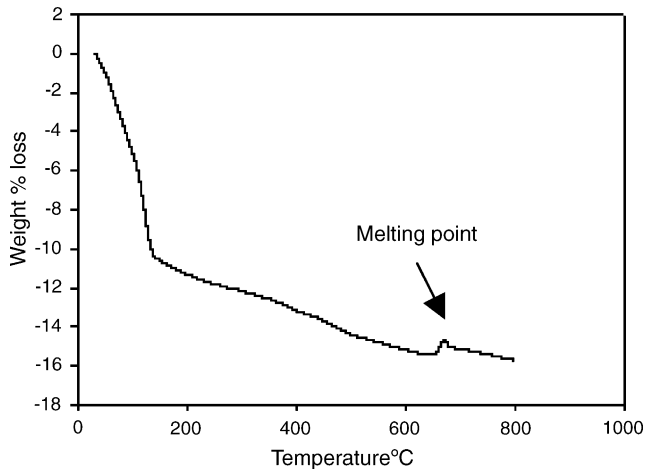


Fig. 3. Thermogravimetric curve of  $V_2O_5$  powders.

in charge storage because of high interaction of the electrode with the electrolyte. Energy dispersive spectrographs showed a small amount of sodium apart from vanadium and oxygen. A surface area of  $7\text{ m}^2\text{ g}^{-1}$  was observed from multi point BET measurement.

#### 4.1. Electrochemical characterization

##### 4.1.1. Effect of electrolytes

Fig. 5 shows cyclic voltammetric curves of  $V_2O_5$  in 2 M KCl at different scan rates. At low scan rates ( $5\text{ mV s}^{-1}$ ), the CV curve shows the near ideal rectangular shape which indicates that charging and discharging took place at a constant rate over the applied voltage range [2]. The small peak on anodic and cathodic sweeps indicates insertion and deinsertion of active  $K^+$  ions respectively. A specific capacitance of  $214\text{ F g}^{-1}$  was obtained for  $V_2O_5$  powders at  $5\text{ mV s}^{-1}$  scan rate. Fig. 6 shows cyclic voltammetric curves of  $V_2O_5$  in 2 M KCl, 2 M NaCl and 2 M LiCl at  $5\text{ mV s}^{-1}$  scan rate. The highest capacitance was observed in 2 M KCl solution. It is interesting to note that  $V_2O_5$  yielded a similar specific capacitance of 114 and  $122\text{ F g}^{-1}$  in 2 M NaCl and 2 M LiCl

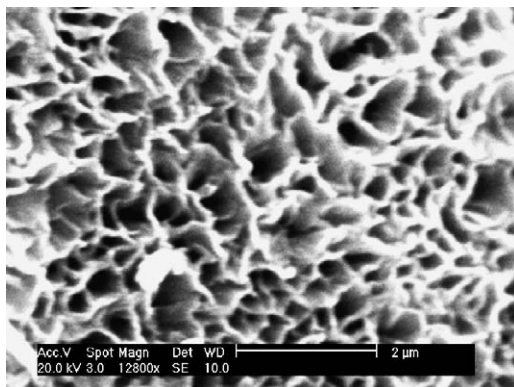


Fig. 4. SEM image of  $V_2O_5$  powders.

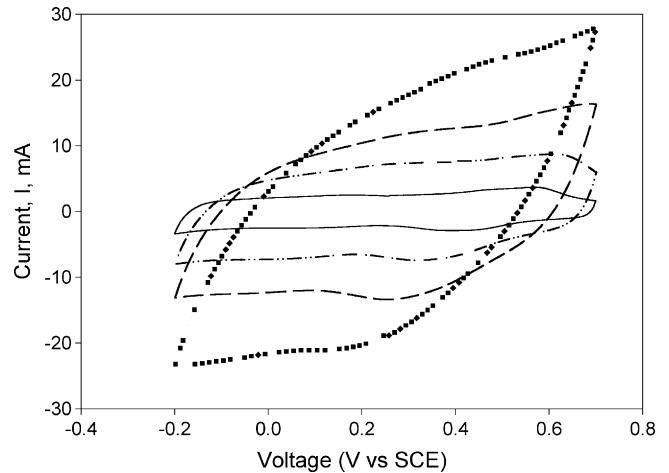


Fig. 5. CV curves of  $V_2O_5$  in 2 M KCl electrolyte at  $20\text{ mV s}^{-1}$  ( $\cdots$ ),  $10\text{ mV s}^{-1}$  ( $---$ ),  $5\text{ mV s}^{-1}$  ( $-\cdot-$ ),  $2\text{ mV s}^{-1}$  ( $\rightarrow$ ) scan rates.

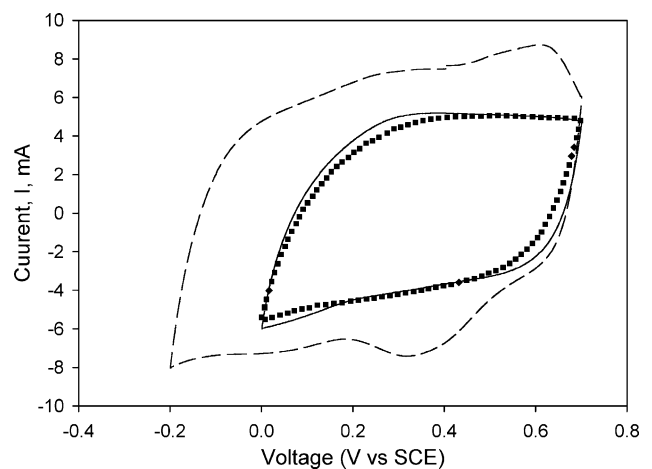
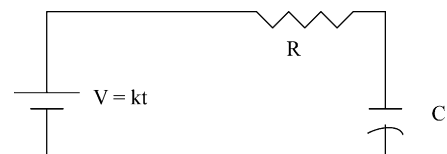


Fig. 6. CV curves of  $V_2O_5$  in 2 M KCl ( $---$ ), 2 M LiCl ( $\rightarrow$ ), 2 M NaCl ( $\cdots$ ) electrolyte at  $5\text{ mV s}^{-1}$  scan rate.

electrolytes respectively, despite the difference in the size of the sphere of hydration of  $Na^+$  and  $Li^+$  ions.

The dependence of voltammetric charge of  $V_2O_5$  in 2 M KCl solution on the scan rate can be understood by the slow diffusion of  $K^+$  ions into the pores of  $V_2O_5$  [15,16]. At high scan rates, diffusion limits movement of  $K^+$  ions due to time constraints and only the outer active surface is utilized for the charge storage. While at lower scan rates all the active surface area can be utilized for charge storage. Variation of capacitance with scan rate and effective series resistance due to electrolyte resistance, electrode resistance and contact resistance can be understood from the following RC circuit. Here capacitance of  $V_2O_5$  is assumed to be constant with the voltage.



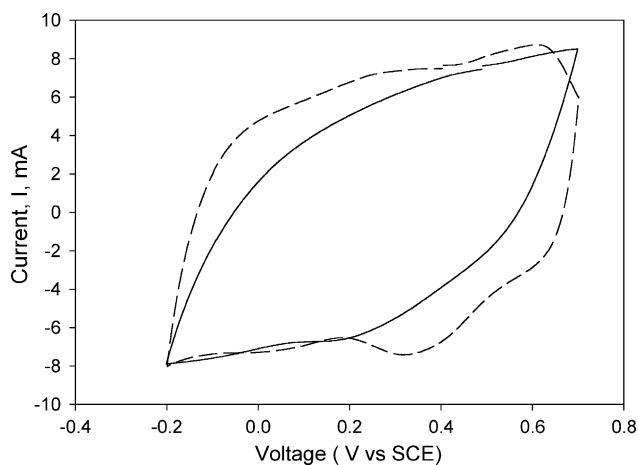


Fig. 7. CV curves of  $V_2O_5$  in 2 M KCl (---), 1 M KCl (—) at  $5 \text{ mV s}^{-1}$  scan rate.

The voltage balance is given by

$$V = V_R + V_c \quad (1)$$

where  $V$  is the voltage of the source,  $V_R$  the voltage of effective resistance comprising of resistance of electrode, electrolyte and contact resistance and  $V_c$  the voltage of the capacitor.

Solving the  $RC$  circuit with voltage input as potential sweep (cyclic voltammetry) with scan rate,  $k$  leads to the following equation [17]:

$$i = kC \left[ 1 - \exp\left(\frac{-t}{RC}\right) \right] \quad (2)$$

where  $i$  is the current generated. It is clear that the nature of the current in the cyclic voltogram is dependent on the time (scan rate) and resistance. At longer times or at a lower effective resistance, Eq. (2) will become

$$i = kC \quad (3)$$

In the case of cyclic voltammetry, Eq. (3) indicates that current will look like a rectangle, which is considered to be an ideal characteristic of a capacitor, when time  $t$  is large or effective resistance is low. In Fig. 5,  $V_2O_5$  shows ideal behavior at the  $5 \text{ mV s}^{-1}$  scan rate when compared to the  $20 \text{ mV s}^{-1}$  scan rate because the former scan rate is four times longer. Fig. 7 shows effect of concentration of KCl on the specific capacitance of  $V_2O_5$  at  $5 \text{ mV s}^{-1}$  scan rate. As can be seen, the figure  $V_2O_5$  showed the ideal capacitor curve in 2 M KCl while in 1 M KCl it is non-capacitative in nature. This can be understood from Eq. (1), since a lower concentration of KCl has a higher electrolyte resistance when compared to 2 M KCl. Higher resistance associated with 1 M KCl results in non-ideal capacitive behavior at the  $5 \text{ mV s}^{-1}$  scan rate. Interestingly, at low scan rates ( $2 \text{ mV s}^{-1}$ ) both electrolytes (1 M and 2 M) yielded the same capacitance. It clearly shows that at lower scan rates, scan rate plays the dominant role.

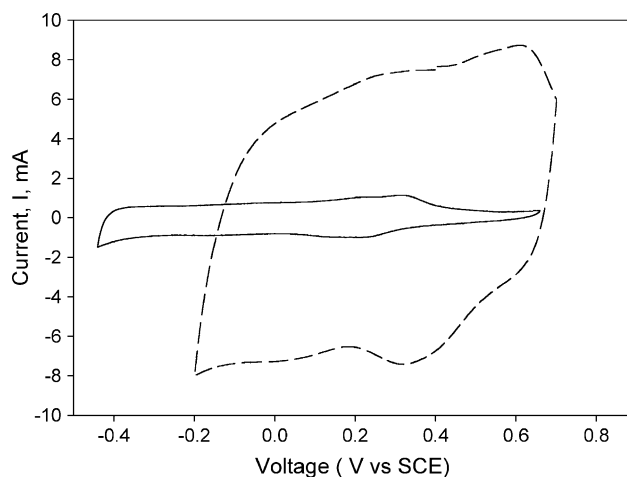


Fig. 8. CV curves of  $V_2O_5$  in 2 M KCl at 1st cycle (---), 100th cycle (—) at  $5 \text{ mV s}^{-1}$  scan rate.

#### 4.1.2. Effect of cycling

Fig. 8 shows the effect of cycling on  $V_2O_5$  in 2 M KCl solution at  $5 \text{ mV s}^{-1}$  scan rate. Specific capacitance faded quickly over 100 cycles. Fading may be due to stress introduced into the structure due to the insertion and deinsertion of  $K^+$  ions. Similar observations were made in our previous study on  $MnO_2$  [2] and we were able to circumvent capacitance fading by doping  $MnO_2$  with Co [18] and by preparing it in a stabilized form [3].  $V_2O_5$  structure needs to be stabilized for cyclic stability. Table 1 shows the specific capacitance of  $V_2O_5$  compared with previously studied  $MnO_2$  and literature  $V_2O_5$  electrode materials. A lower specific capacitance of the present  $V_2O_5$  when compared to the literature may be due to the difference in the preparation conditions and the physical nature of the material (amorphous/crystalline). One important issue to notice in this study is the preparation of the novel nano porous honeycomb type structure. These types of structures are highly preferred in energy storage applications. Deeper understanding of preparation conditions and optimizing can lead to new porous materials which can be an excellent candidate for an electrochemical capacitor. The study of the relation between preparation conditions and the morphology of  $V_2O_5$  powers are under way.

Table 1  
Comparison of specific capacitance of  $V_2O_5$  with previously studied  $MnO_2$  and  $V_2O_5$  from literature at the scan rate of  $5 \text{ mV s}^{-1}$

Electrode material	Electrolyte	Specific capacitance ( $\text{F g}^{-1}$ )	Reference
$V_2O_5$	2 M KCl	214	Present study
$V_2O_5$	2 M KCl	364	[11]
$MnO_2$	2 M NaCl	130	[2]
Stabilized $MnO_2$	2 M NaCl	110	[3]
Co stabilized $MnO_2$	1 M NaCl	110	[18]

## 5. Conclusions

A nano porous layer structured  $V_2O_5$  was prepared using sol–gel method.  $V_2O_5$  showed the highest capacitance in 2 M KCl electrolyte when compared to other electrolytes such as NaCl and LiCl. It yielded maximum specific capacitance of  $214 \text{ F g}^{-1}$  in 2 M KCl electrolyte. Concentration of KCl showed strong dependence on specific capacitance at higher scan rates. Fading of capacitance was observed after over 100 cycles. Fading may be due to change in  $V_2O_5$  structure resulted during the insertion and deinsertion of  $K^+$  ions.

## Acknowledgement

The authors are thankful for the financial support provided by National Science Foundation grant no. ECS-0099853.

## References

- [1] B.E. Conway, *Electrochemical Supercapacitors*, Kluwer Academic/Plenum Publishers, New York, 1999.
- [2] Ravinder N. Reddy, Ramana G. Reddy, *J. Power Sources* 124 (1) (2003) 330.
- [3] Ravinder N. Reddy, Ramana G. Reddy, *J. Power Sources* 132 (1–2) (2004) 315.
- [4] H.Y. Lee, S.W. Kim, H.Y. Lee, *Electrochem. Solid-State Lett.* 4 (2001) A19.
- [5] C.C. Hu, C.C. Wang, *J. Electrochem. Soc.* 150 (2003) A1079.
- [6] R.N. Reddy, R.G. Reddy, *Electrochemical capacitor and hybrid power sources*, in: R.J. Brodd, D.H. Doughty, K. Naoi, M. Morita, C. Nanjundiah, J.H. Kim, Nagasubramanian (Eds.), PV 2002-7, The Electrochemical Society Proceedings Series, Pennington, NJ, 2002, p. 197.
- [7] Ravinder N. Reddy, Ramana G. Reddy, in: D. Chandra, R.G. Bautista, L. Schlapbach (Eds.), *Advanced Materials for Energy Conversion*, vol. II, TMS, Warrendale, 2004, p. 355.
- [8] Y.U. Jeong, A. Manthiram, *J. Electrochem. Soc.* 149 (2002) A1419.
- [9] J. Suryanarayan, M.S. Thesis, The University of Alabama, 2001.
- [10] S.C. Pang, M.A. Anderson, T.W. Chapman, *J. Electrochem. Soc.* 147 (1997) 444.
- [11] H.Y. Lee, J.B. Goodenough, *J. Solid State Chem.* 148 (1999) 81.
- [12] Ravinder N. Reddy, Ramana G. Reddy, *Power sources for transportation applications*, in: A.R. Landgrebe, T.Q. Duong, A.J. Salking, K. Zaghbi, B.S. Battaglia, Z. Ogumi, I.B. Weinstock, *Proceedings of the International Symposium, PV 2003-24*, The Electrochemical Society Proceedings Series, Pennington, NJ, 2004, p. 213.
- [13] T. Kudo, Y. Ikeda, T. Watanabe, M. Hibino, M. Miyayama, H. Abe, K. Kajita, *Solid State Ionics* 152–153 (2002) 833.
- [14] F. Huguenin, E.M. Girotto, R.M. Torresi, D.A. Buttry, *J. Electroanal. Chem.* 536 (2002) 37.
- [15] S. Ardizzone, G. Fregonara, S. Trassatti, *Electrochim. Acta* 35 (1990) 263.
- [16] M. Toupin, T. Brousse, D. Belanger, *Chem. Mater.* 14 (2002) 3946.
- [17] A.J. Bard, L.R. Faulkner, *Electrochemical Methods: Fundamentals and Applications*, 2nd ed., Wiley, New York, 2001.
- [18] Ravinder N. Reddy, R.G. Reddy, *J. New Mater. Electrochem. Syst.*, 7 (2004) 317.